Research & Reviews: Journal of Material Sciences e-ISSN: 2321-6212

A Computational Study of Adsorption of Noxious Gases on the Activated Carbon Surfaces

Akhtar Hussain*

Department of Science and Technology, Pakistan Institute of Nuclear Science and Technology (PINSTECH), Islamabad, Pakistan

Research Article

Received: 19-Apr-2024, Manuscript No. JOMS-24-132664; **Editor assigned:** 22-Apr-2024, PreQC No. JOMS-24-132664 (PQ); **Reviewed:** 06-May-2024, QC No. JOMS-24-132664; **Revised:** 04-Mar-2025, Manuscript No. JOMS-24-132664 (R); **Published:** 11-Mar-2025, DOI: 10.4172/2321-6212.13.1.001

***For Correspondence:** Akhtar Hussain, Department of Science and Technology, Pakistan Institute of Nuclear Science and Technology (PINSTECH), Islamabad, Pakistan

Email: ahmohal@yahoo.com

Citation: Hussain A. A Computational Study of Adsorption of Noxious Gases on the Activated Carbon Surfaces. RRJ Mater Sci. 2025;13:001.

ABSTRACT

Adsorption capacity of Activated Carbon (AC) for Ammonia (NH_3), Nitric Oxide (NO), Carbon Monoxide (CO) and Iodine (I) molecules employing DFT is investigated. 2-ring, 3-ring, 6-ring and 9-ring carbon structures are used as adsorbent surfaces. These models are investigated by creation of defects on surfaces and functionalization with hydrogen. Planar and non-planar mode adsorption is considered. The planar-mode interactions have much higher adsorption energy and shorter connecting distances than non-planar mode adsorption. The adsorption properties dependent on the adsorption mode, surface size, hydrogenation and whether the system is perfect or defected. Defect produced at the central position of the surface helps to bind the adsorbent more strongly. However, the adsorption energy varies depending upon various factors and does not follow any consistent rule. The smaller sized structures are favorable for CO and NO capture. Conclusively, AC is promising material for adsorption of the noxious gases.

Keywords: DFT; Activated carbon; Adsorption; Noxious gases; NH_3; CO; NO

INTRODUCTION

Inorganic and organic compounds pollutants in addition to others heavy metals and toxic like SO_x, H_2S, NO_x, CO, I and NH_3 caused by industrialization, urbanization at large scale and increase in world population have become a source of soil, air and water pollution badly effecting human life and environment [1]. Controlling such pollution has becoming a challenge to keep the human society environmentally clean. To circumvent pollution effectively, among the others, adsorption process is simple and easy way to employ, does not produce any un-wanted substances and is thus attractive and used widely [2,3].

The adsorbent must be competent enough of having large surface area, pore volume and appropriate functionalities to circumvent the pollutants effectively and successfully. The advancement in this field has caused to develop a variety of such materials with varying desired efficiency in removing the toxic pollutants from soil, water and air but out of them Activated Carbon (AC), carbon nanotubes and fullerene are thermally stable and show good adsorption properties [4-9]. The source of AC is solid, porous and black carbonaceous martial. AC is obtained after processing these materials. Precursors of AC include wood, coconut shells and nut shells or of all ranks of coal i-e all have botanical origin. AC is a favorable material for adsorption of noxious gases owing to its remarkable characteristics of large surface area (500 to 3000 meter square per gram), surface chemistry, active surface and pore structure.

As far as the structure of AC is concerned, the recent experimental observations report it like fullerene construction. Its curved fragments contain hexagons, pentagons and other non-hexagonal rings. The first observations in this regard were understood and reported by Rosalind Franklin in 1950 [10].

The AC is a very useful material with potential applications in different areas including industry. The AC play vital role for gas storage, noxious waste and odor removal due to its large surface area and pore structure. Further applications include its use in nuclear industry, gas separation, catalysis, gas cleaning, metal extraction, water distillation and chemical purification. It has also uses in fuel cells and medicinal area [11]. The most of its applications for practical purposes route through adsorption process. The AC can be more useful if its adsorption properties are enhanced. Various atoms like O, H, N, S can be employed as functional material to serve the purpose. Different experimental techniques are used for accomplishment [12-14]. As reported, the Eads of CO, NO and NO_2 molecules on graphene enhanced due to creation of defects in adsorbent surface. The structure of graphene is similar to AC [15].

CO, NO, I and NH_3 have side effects and effect the human healthy life in one or the other way. To have detailed overview about the adsorption properties of CO, NO, I and NH_3 pollutants, we carried out investigations on different activated carbon structures. These AC surfaces of varied size *i.e.*, 2-6 ring models have been considered for computation. These models have been constructed keeping in view the experimental observations reported by Harris et al. In order to have investigation on such models close to experimentally determined ones, we created defects to have pentagonal, squarely and heptagonal configurations in addition to hexagonal surfaces. We have functionalized the surfaces with H to compute the impact of hydrogen on adsorption properties of these noxious gases.

The investigations have been carried out in order circumvent the noxious gases CO, NO, I and NH_3 by the process of adsorption on activated carbon. After experimental determination and reporting the evidence regarding the hexagon, pentagon, heptagon angular rings and other structures, we have computationally observed the adsorption properties. These configurations mimic graphene like structures. For the purpose of adsorption of gases, surface area and surface chemistry play a crucial role for efficient and effective adsorption and in case of AC surfaces, we have these. In order to have comprehensive view, we have considered the systems size, effect of creation of defects, mode of adsorption (planner, non-planner), adsorption site and functionalization of the surfaces with H-atoms. The results have clearly shown that some configuration are highly reactive and adsorb the noxious gases chemically. DFT can be effectively employed to compute the adsorption energies of gases on micro porous material like activated carbon. The results obtained are discussed in the following sections.

MATERIALS AND METHODS

Computational details

Vienna Ab-initio Simulation Package (VASP) to perform the DFT calculation which uses the iterative technique for the solution of Kohn-Sham equations in a plan-wave basis set [16,17]. All plane-waves with a kinetic energy below or equal to 450 eV were included in the calculation. Generalized Gradient Approximation (GGA) is used for the calculation of exchange-correlation energy [18]. The Projector-Augmented Wave (PAW) method developed by Blöch described the electron-ion interaction of carbon atoms with gas atoms [19].

For the computation we used different sized super cells (because the size of the surfaces is different) keeping in view the trade-off between computational costs and to avoid interaction between the neighboring molecules in repeating cells in the periodic systems. For 2-ring and 3-ring carbon structures the fullerene like structures of activated carbon were modeled by giving relative coordinates of carbon atoms in a $10 \times 10 \times 10$ Å^3 cubic unit cell with C-C distance of 1.42 Å. For the hydrogenated 3-ring models (with and without defects) and carbon structures having 6 rings, relative co-ordinates of carbon atoms are modeled in $15 \times 15 \times 15$ Å^3 cubic unit cell. In all cases, $(1 \times 1 \times 1)$ k-point meshes were automatically generated using the Monkhorst-pack method [20].

All atoms of the systems were relaxed during optimization process, using the RMM-DIIS algorithm. In this method, the forces on the atoms and the stress tensor are used to determine the search directions for finding the optimized equilibrium positions of atoms. Geometry optimizations were stopped when all the forces were smaller than 0.01 eV/Å. The non-spin polarized calculations were performed to determine the ground state energy of the bare carbon slabs and after the adsorption of the molecules of the gases on these slabs within Generalized Gradient Approximation (GGA). Some structures were re-optimized employing spin polarized calculations; nevertheless, differences in adsorption energies and geometries were subtle and thus ignorable.

The adsorption energies are calculated using the equation (1) given in reference.

$$E_{ads}=E_{substrate+adsorbate}-(E_{gas\ phase\ energy\ of\ adsorbate}+E_{substrate}) \qquad (1)$$

Where $E_{substrate+adsorbate}$ is the total energy of the adsorbate and substrate system, $E_{substrate}$ is the energy of the substrate without adsorbents on the surface and E_{gas} phase energy of adsorbate is the energy of the isolated CO, NO, I or NH_3 molecule in gas phase. The negative adsorption energy indicates an exothermic process.

RESULTS AND DISCUSSION

The hazardous gases I, NH_3, CO and NO have been taken into consideration to determine their geometrical and adsorption properties on activated carbon. The experimentally reported AC are mostly rings shaped (using SEM, hexagonal, pentagonal as well as heptagonal rings have been observed) so the names of these structure follow from that concept. For understanding these configurations are named after the numbers of rings present in a particular super cell, hence the 2-ring, 3-ring and 6-ring configurations. The defects created at edge sides get repaired changing hexagonal rings into pentagonal ones normally during optimization procedure. The missing structures in order (comprising of 4, 5, 7 and 8-rings) were also considered but the geometries of their bare structures were not stable during optimization. The description order followed is Iodine, ammonia, nitric oxide and carbon monoxide.

Iodine adsorption on AC

Adsorption of iodine on 2-ring AC structure

Planner mode: Iodine strongly interacts with the 2-ring surfaces presented in Figure 1 accompanying substantial variation in Eads. On iodine adsorption the defected 2-ring structure is modified as one of the ring acquires penta shape after optimization as shown in Figure 1a, initially penta of defected 2-ring comprises of square and triangular geometry joined together.

Figure 1. Interaction of iodine with 2-ring AC structure. In (a) defected 2-ring (which during optimization deforms into benzene like hexagonal ring and a pentagonal one) model is presented. In (b) part hydrogenated 2-ring and in (c) H insertion with defect is given.

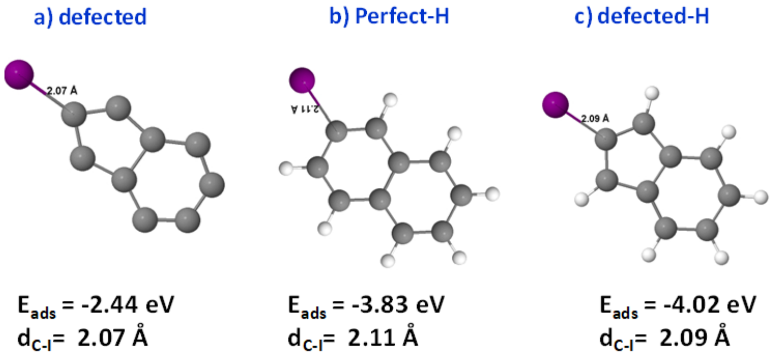

Defected 2-ring slab shows strong bonding having E_{ads}=-2.44 eV and the resultant separation between iodine and carbon slab is 2.07 Å. Impregnation of hydrogen with 2-ring AC has enhanced the E_{ads} to -3.83 eV showing even stronger cooperative relation between iodine and hydrogenated surface as illustrated in Figure 1b. In accord with our anticipation creation of defect in impregnated 2-ring AC model has further enhanced the E_{ads} (-4.02 eV) in agreement with lower distance as depicted in Figure 1c advocating for the most favorable configuration.

Adsorption of iodine on 3-ring AC: Iodine interacts with all the structures discussed for 3-ring configurations. Adsorption properties of iodine in planar and non-planar mode are discussed below.

Non-planar mode of interaction: A central position of the surface is chosen to adsorb I in non-planar mode. The surface goes under variation in geometry as I is placed upon the surface. Eads of I varies significantly on creation of defect in addition to observed small increase due to hydrogenation (Figure 2d). Thus clean defected model with E_{ads} -0.71 eV of I is preferred configuration.

Figure 2. Interaction of iodine with 3-ring AC structures at surface central top site is presented. In order (a-d) represent perfect, defected, perfect hydrogenated and defected hydrogenated configurations.

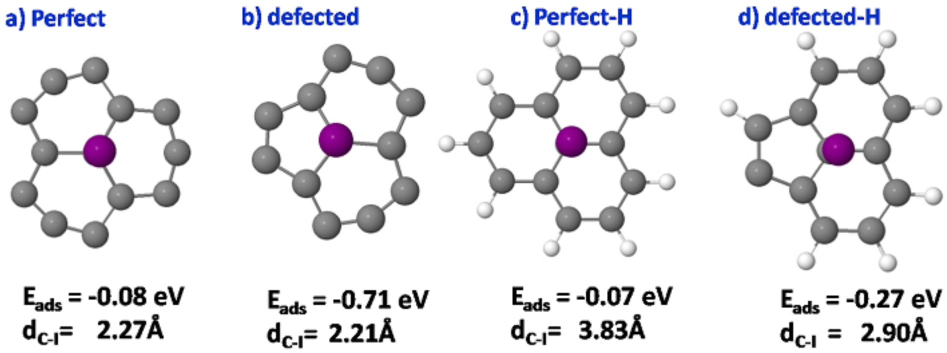

Planar mode interaction: As we observed for the surfaces consisting of 2-rings, iodine shows strong chemical bonding with all the structures when lying in the plane of 3-ring AC structures. The calculated results are illustrated in Figure 3. Iodine is found to adsorb with E_{ads} varying between -2.97 to -4.06 eV. This variation occurs in E_{ads} due to changing the binding position with defected ring or as a result of hydrogenation. The hydrogenated structures here always cause to increase in E_{ads}. The highest E_{ads} achieved is in agreement with the lowest (I-C) bond length as shown in the last part of the Figure 3.

Figure 3. Depicts planar mode interaction of iodine with 3-ring AC structure. In parts a-d in order interaction with bare perfect, defected, perfect hydrogenated and defected hydrogenated surfaces is shown.

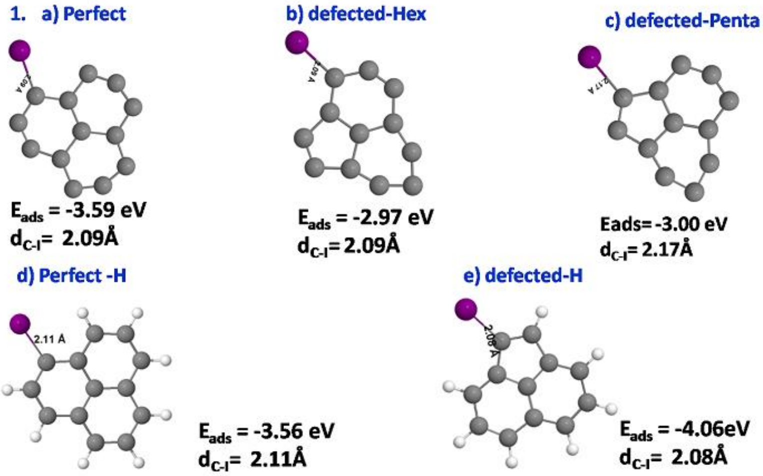

Adsorption of Iodine on 6-ring AC: Iodine adsorption on this surface in non-planar and planner mode is depicted in different parts of Figure 4. It can be observed that as the ring structure increases the top mode for iodine adsorption has repulsive interaction which is the most inauspicious mode for adsorption.

On replacement of I with central C-atom of the surface make bonds longer than usual C-C bonds. This becomes a case of substitution/doping rather than simple adsorption because iodine remains slightly above the plane of C-atoms. However, relative to clean optimized surface, the system is stabilized by -2.18 eV. The planar coordination of iodine with surface also shows strong interaction as depicted in Figure 4c, which is also the most favored configuration. Additionally, this configuration is in agreement with shorter I-C bond distance (2.08 Å).

Figure 4. Interaction of iodine with 6-ring AC structure. a) adsorption of iodine in non-planar mode, b) adsorption when defect is created at the center of 6-ring and I is placed above the defected site and finally c) represents planar mode configuration.

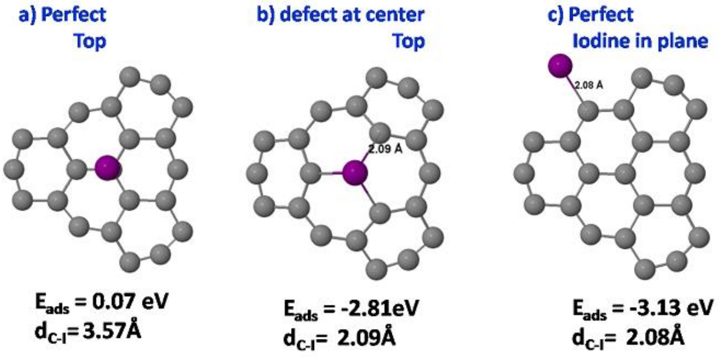

Experimental observations are about iodine adsorption and report impregnation of I in pores but cannot be directly compared with our results (Figure 5).

Figure 5. Adsorption energies *vs.* bond length graph for iodine.

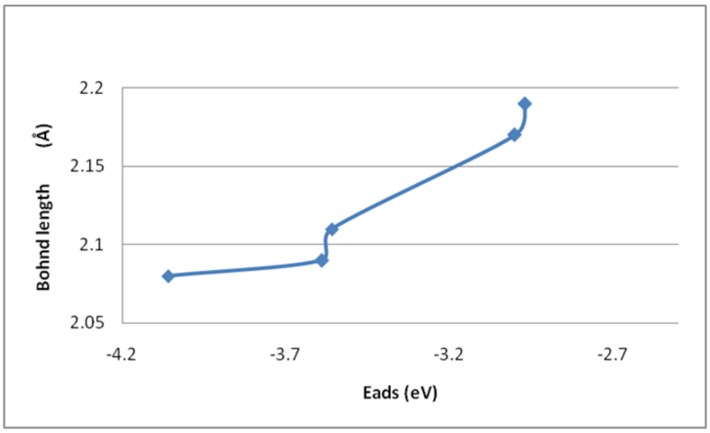

NH_3 adsorption on AC

NH_3 molecule shows inconsistent adsorption properties in planar and non-planar configurations on different AC structures, showing more complicated adsorption mechanism than the other molecules reported above.

Adsorption of NH_3 on 2-ring AC structure: Adsorption of NH_3 on activated carbon 2-ring structure remains repulsive in either case of defected, perfect hydrogenated and defected hydrogenated models as shown in Figure 6. None of the surfaces is good enough to accommodate the molecule.

Figure 6. Interaction of NH_3 in planar mode with a) defected, b) hydrogenated and c) defected and hydrogenated 2-ring model surfaces.

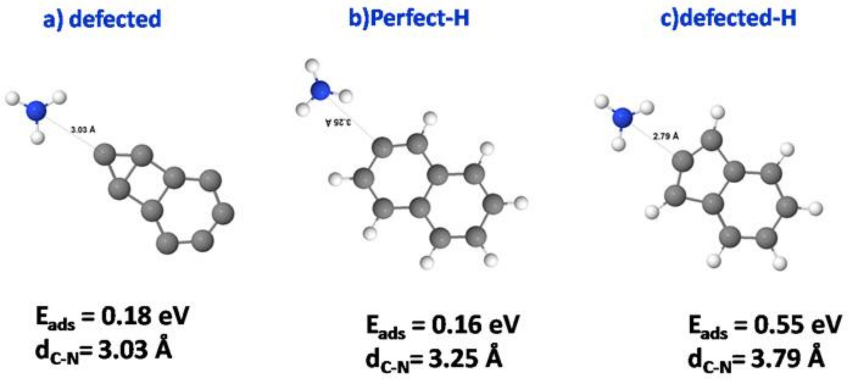

Interaction of NH_3 with 3-ring AC: Two modes of adsorption of NH_3 on 3-ring model are discussed here. We've taken a non-planar mode in which NH_3 is placed above the 3-ring structure at different configurations as in planar mode in which adsorption of molecule takes place in the same plane where the adsorbate lies and in non-planar mode where molecule lies above the surface.

Interaction in non-planar mode: Ammonia has showed no binding with any of the system leaving the system unpurturbed illustrated in Figure 6 in which interaction in non-planar mode is shown. Thus non-planar mode is not favorable for ammonia adsorption (Figure 7).

Figure 7. Different configurations presented respectively in a-d give the interaction of NH_3 with perfect, defected, perfect-hydrogenated and defected hydrogenated ring of 3-ring AC surfaces in non-planar adsorption of NH_3 on central top location.

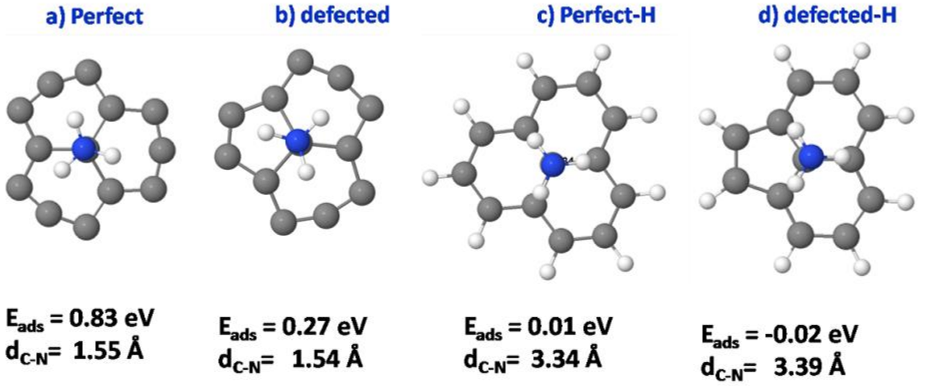

The interaction in non-planar mode of adsorption of NH_3 on perfect, defected, defected hydrogenated and perfect hydrogenated 6-ring surfaces as shown in Figure 6 (a-d), remains either repulsive or negligibly small attractive.

Interaction in planar mode: As it can be determined from Figure 7 that 3-ring AC surfaces are better regarding adsorption of NH_3 relative to similar surfaces comprising of 2-ring models. The highet Eads of -2.34 eV observed for NH_3 connecting through N-atom to C-atom of penta formed ring after creation of defect as depicted in Figure 8. The N-atom is found close to the surface at bond length of 1.49 Å. H insertion has counter response, hence does not help to adsorb NH_3 (Figure 9).

Figure 8. Different configurations presented respectively in a-d give the interaction of NH_3 with perfect, defected, perfect-hydrogenated and defected hydrogenated ring of 3-ring AC surfaces.

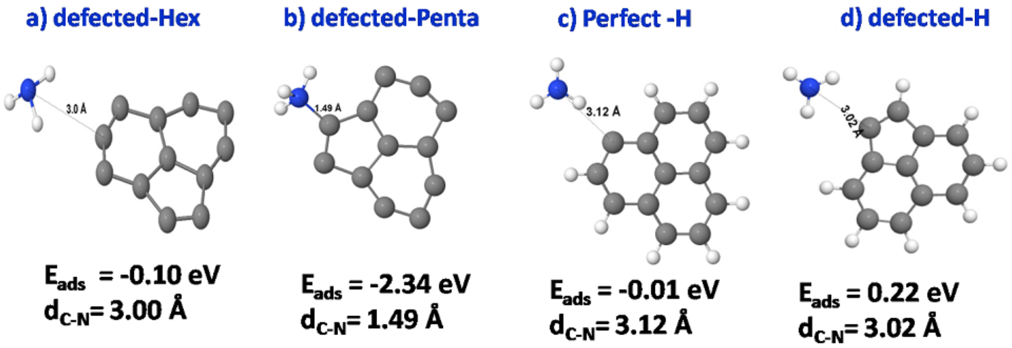

Figure 9. Bond length variation with adsorption energies of NH_3 on different slabs of 3-ring AC in planar mode.

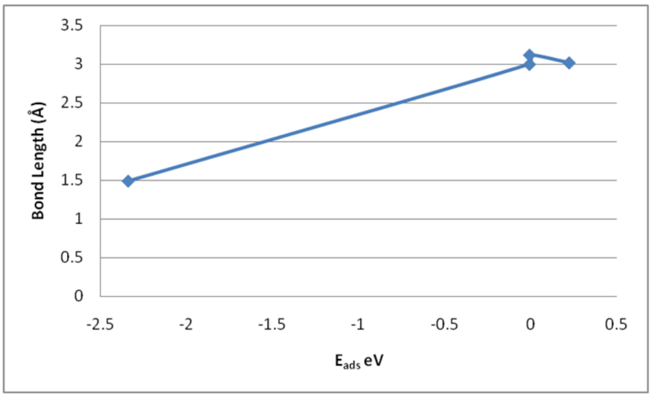

Interaction of NH_3 with 6-ring AC: As we have seen enlargement surface size caused to enhance the interaction of NH_3 with AC surfaces. Therefore, we also tried 2 surfaces with different modes for investigation. As expected, NH_3 exhibited strong interaction with the surface in planar mode of coordination given in Figure 10. The N-C bond distance is found very small (1.47 Å) in agreement with higher binding energy.

Figure 10. Interaction of NH_3 with bare 6-ring a) in non-planar mode b) in planar mode.

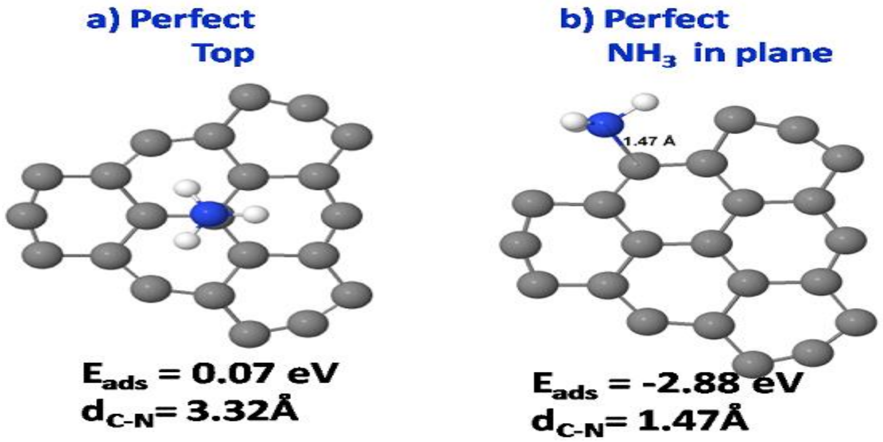

Guo et al., carried out experimental investigations for adsorption tests for a wide range of temperatures suggested combined physisorption and chemisorption of NH_3. Desorption tests at the same temperature as adsorption and at an elevated temperature were carried out to confirm the occurrence of chemisorption due to the interaction between NH_3 and some oxygen functional groups *via* hydrogen bonding. The observations are in line with our results indicating both week and strong adsorption. Water impregnation enhances NH_3 binding.

Adsorption of NO on different activated carbon models

Adsorption of NO on 2-ring AC structure: The interaction of NO with various surface models as shown in Figure 11 has been examined. All the planar model configurations show that NO shows significant adsorption energy with all the surfaces. However, the variation in E_{ads} (-1.33 to -1.71 eV) depends upon whether surface is defected, hydrogenated or not. The lowest E_{ads} is computed for perfect hydrogenated and the highest for defected hydrogenated surface. It is important to note that NO always make tilted adsorption binding through its N-atom with C-atom of the surfaces. Bond distances (1.43 to 1.37 Å) are in agreement with variation in E_{ads}.

Figure 11. Interaction of NO in planar mode of adsorption with (a) defected, (b) perfect hydrogenated and c) after vacancy creation and hydrogenation.

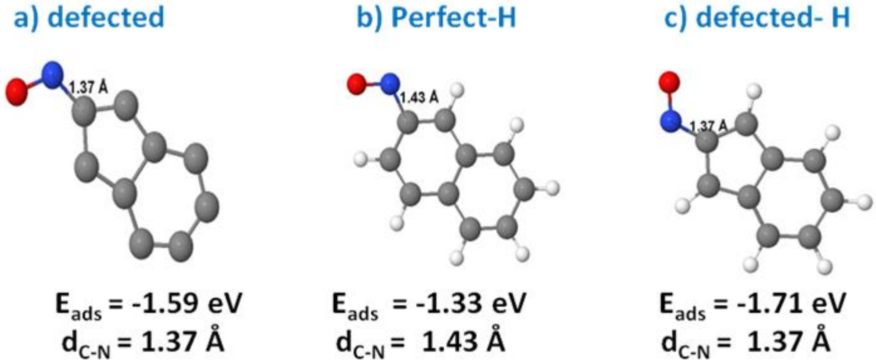

Adsorption of NO on 3-ring AC structure: NO adsorption studied on 3-ring AC models shown different behavior by yielding substantial change in E_{ads} with creation of defect and insertion of H. Additionally, with bigger size sudden fall in E_{ads} is in contrast to as observed in case of NH_3 where E_{ads} enhances with surface size increase. NO showed very weak interaction with the bare slab 3-ring model with and without defect. Yet the NO has modified the perfect 3-ring slab during optimization as depicted from Figure 12. As two hexagonal rings transformed into one heptagon and one pentagon ring structure. Such configurations are observed experimentally.

Figure 12. Interaction of NO with (a) pentagonal with one heptagon, (b) hexagonal, (c) pentagonal with reaming 2 hexagons, (d) hydrogenated hexagonal and (e) hydrogenated pentagonal ring, 3-ring AC structures in planar mode are shown.

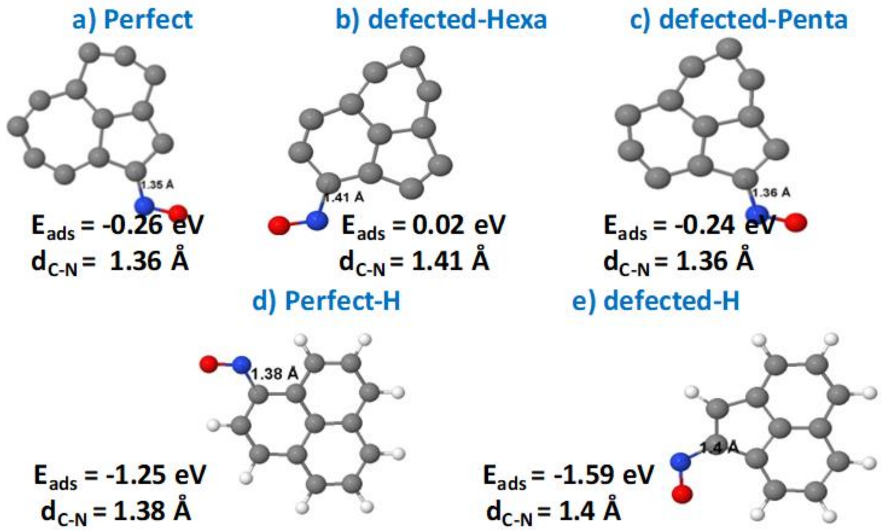

In case of NO, H insertion has played very significant role towards its adsorption. On perfact hydrogenated 3-ring surface the E_{ads} of NO rises to -1.25 eV, which becomes -1.59 eV if similar site is computed by creating a defect *i.e.*, NO association with pentagon. H insertion not only enhances the binding energy of NO with AC but also preserves the structure of AC rings. This can clearly be seen by comparing the naked and hydrogenated surfaces.

Kunjie et al., have investigated NO adsorption on Pt and Pd decorated carbon nano tube surfaces using DFT at GGA= PW91 level and found the strong adsorption of NO adsorbed on Pt/Pd. NO has been discussed to be adsorbed on ACs in reference. Nevertheless, reported AC surfaces are similar to those our ones but direct comparison of our observations with reported in this study is not appropriate.

Adsorption of CO on different activated carbon models

CO bonding has been discussed only for 2-ring and 3-ring AC structures as in planar mode, whilst optimization during adsorption of CO, the structures containing 6 and 9-ring do not remain stable.

Adsorption of CO on 2-ring AC structure: The surface shown in Figure 13 (a) and (c) only differ in hydrogenation of the later. However, comparison in E_{ads} of CO for both the configurations shows a drastic increase in E_{ads} due to H insertion. The interaction of CO with naked AC surface is also significant, while CO binds with pentagonal ring (-1.8 eV), however, does not interact at all with heptagonal configuration. Rather interactive relation is feebly repulsive. Thus 2-ring structure AC containing pentagonal naked/hydrogenated surfaces are very good materials for CO adsorption.

Figure 13. Interaction of CO in planar mode with a) defected surface forming one pentagon, b) hydrogenated surface and the molecule adsorbed with heptagon and c) where the molecule interacts with pentagonal ring with H-atoms adsorbed with remaining C-atoms.

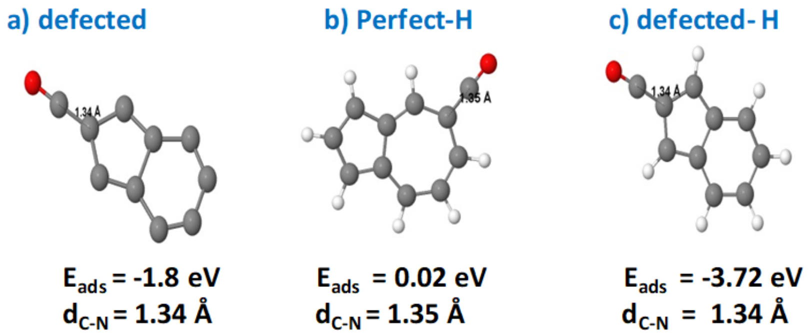

Adsorption of CO on 3-ring AC structure: On use of 3-ring surface it can be seen that CO adsorption causes to distort the surface structure significantly. The situation becomes more interesting when H is incorporated in this surface. As illustrated in Figure 14b, another hexagonal ring is converted into pentagon and CH_2 attached with the ring. Both the surfaces are good enough to chemisorb the CO molecules. On naked and hydrogenated surfaces, respective E_{ads} of CO is -2.56 and -2.77 eV illustrated in Figure 14. None of the other geometry remains stable in planar mode with CO interaction except two models discussed here. Both defected models with and without hydrogen are good for CO adsorption.

Figure 14. Pentagonal interaction of CO with (a) bare and (b) hydrogenated 3-ring AC surfaces. After removal of C-atom pentagonal geometry is formed.

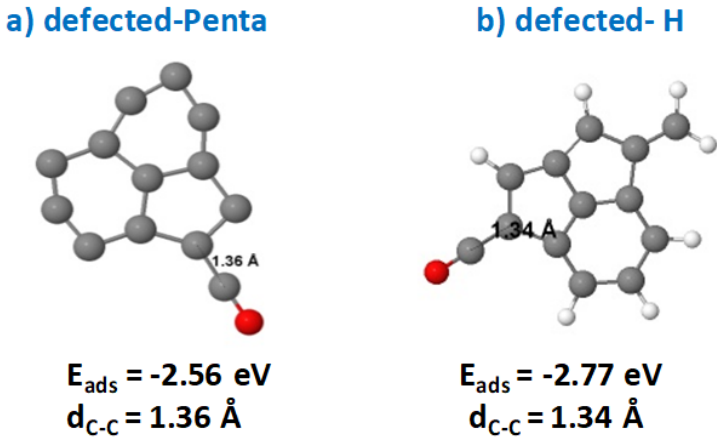

Cao and co-workers have investigated CO adsorption on Pt and Pd decorated carbon nano tube surfaces using DFT at GGA=PW91 level and found the strong adsorption of CO coordinating with Pt/Pd. Experimental observations also report adsorption of CO in the form of impregnation in reference. However, we could not find any direct relevance of our results with those reported in literature.

CONCLUSION

We have performed DFT calculations on different structures of AC to evaluate the adsorption properties of NH_3, NO, CO and iodine on these structures. The effect of creation of defect in the surface, structure size and insertion of hydrogen on adsorption energy has been examined. There are very less points which are consistent for all the adsorbates studied. Thus important conclusions are described separately for each adsorbate and finally the common observations are summarized.

Iodine adsorbs strongly on all the reported configurations. The E_{ads} varies from 0.07 to -4.06 eV depending upon mode of adsorption, site, functionalization of structure with H etc. We have observed that adsorption energy increases by creation of defect and insertion of hydrogen in AC surfaces in planar mode. The increase in ring size has increasing trend in adsorption energies up to 3-ring but afterwards the trend is opposite. In non-planar mode, the adsorption energy increases by creating defect and inserting hydrogen simultaneously in the ring structure.

Ammonia has showed very weak interaction in both the modes of adsorption up to 3-ring structures. Whereas bare 6-ring surface is found to be the most favorable configuration for NH_3 adsorption in planar-mode yielding Eads of -2.73 eV. NH_3 is not stable on any surface in non-planar mode of adsorption.

NO has strong bonding with smaller AC structures like 2-ring model. Hydrogenation has enhanced the interaction both for 2-ring and 3-ring surfaces. Insertion of defect and hydrogen simultaneously, causes to increase the adsorption energy on these systems. Interaction of NO with bigger structures has distorted the geometry in planar mode.

CO does not interact in non-planar mode. However, with defected and hydrogenated defected models in planar mode, strong CO adsorption is found. CO has completely modified the hydrogenated structures in planar mode. Bigger structures are not stable when CO interacts.

The lack of consistency in adsorption properties of different molecules is observed on change of size, mode, H insertion and defect creation. Adsorption properties are strongly dependent on the configuration, size and system of AC models. Usually, the most stable structures are found when adsorbents lie in side by side geometry with AC surfaces. Hydrogenation has enhanced the molecule affinity with the AC structure except NH_3 in planar configuration. Summarily it can be safely concluded that activated carbon is very good material for adsorption of noxious gases.

ACKNOWLEDGEMENT

We acknowledge the support of MIS at PINSTECH, and PIEAS, Islamabad, with regards to providing the computational resources. This work has been supported by Pakistan Atomic Energy commission.

CREDIT AUTHORSHIP CONTRIBUTION STATEMENT

Dr. Akhtar Hussain gave idea of the research, contributed towards calculations, prepared manuscript and supervised the research. Dr. Saqib Javed helped with calculations and the preparation and corrections of the manuscript.

REFERENCES

1. Wang S, et al. Adsorptive remediation of environmental pollutants using novel graphene-based nanomaterials. Chem Eng J. 2013;226:336-347.
2. Wang S, et al. Natural zeolites as effective adsorbents in water and wastewater treatment. Chem Eng J. 2010;156:11-24.
3. Dubey SP, et al. Utility of adsorbents in the purification of drinking water: a review of characterization, efficiency and safety evaluation of various adsorbents. J Environ Biol. 2009;30:327-332.
4. Ren X, et al. Carbon nanotubes as adsorbents in environmental pollution management: a review. Chem Eng J. 2011;170:395-410.
5. Gupta SS, et al. Adsorption of heavy metals on kaolinite and montmorillonite: A review. Phys Chem Chem Phys. 2012;14:6698-6723.
6. Jjagwe J, et al. Synthesis and application of granular activated carbon from biomass waste materials for water

treatment: A review. J Bioresour Bioprod. 2021;6(4):292-322.

7. Rao GP, et al. Sorption of divalent metal ions from aqueous solution by carbon nanotubes: a review. Sep Purif Technol. 2007;58:224-231.
8. Wang S, et al. A comparative study on the adsorption of acid and reactive dyes on multiwall carbon nanotubes in single and binary dye systems. J Chem Eng Data. 2012;57:1563-1569.
9. Saleem J, et al. Production and applications of activated carbons as adsorbents from olive stones. Biomass Convers Biorefin. 2019;9:775-802.
10. Harris PJ, et al. Imaging the atomic structure of activated carbon. J Phys Condens Matter. 2008;20:362201.
11. Mestre AS, et al. Waste-derived activated carbons for removal of ibuprofen from solution: role of surface chemistry and pore structure. Bioresour Technol. 2009;100:1720-1726.
12. Sultana M, et al. A review on experimental chemically modified activated carbon to enhance dye and heavy metals adsorption. Clean Eng Technol. 2022;6:100382.
13. Borchardt L, et al. Toward a molecular design of porous carbon materials. Mater Today. 2017;20:592-610.
14. Bandosz TJ, et al. On the reactive adsorption of ammonia on activated carbons modified by impregnation with inorganic compounds. J Colloid Interface Sci. 2009;338:329-345.
15. Zhang YH, et al. Improving gas sensing properties of graphene by introducing dopants and defects: A first-principles study. Nanotechnology. 2009;20:185504.
16. Kresse G, et al. Efficiency of ab-initio total energy calculations for metals and semiconductors using a plane-wave basis set. Comput Mater Sci. 1996;6:15-50.
17. Kresse G, et al. Efficient iterative schemes for ab initio total-energy calculations using a plane-wave basis set. Phys Rev B Condens Matter. 1996;54:11169-11186.
18. Perdew JP, et al. Generalized gradient approximation made simple. Phys Rev Lett. 1996;77:3865-3868.
19. Blochl PE, et al. Projector augmented-wave method. Phys Rev B Condens Matter. 1994;50:17953-17979.
20. Monkhorst HJ, et al. Special points for Brillouin-zone integrations. Phys Rev B. 1976;13:5188-5192.